JOURNAL OF MATERIALS SCIENCE 35 (2000) 5973–5980

Effects of composition and sintering time on liquid phase sintered Co-Cu samples in microgravity

YUBIN HE, SAIYIN YE, J. NASER
Department of Chemical and Materials Engineering, University of Alabama in Huntsville, Huntsville, Alabama 35899, USA

J. CHIANG
Nextek Inc., Madison, Alabama 35758, USA

J. E. SMITH, JR.
Department of Chemical and Materials Engineering, University of Alabama in Huntsville, Huntsville, Alabama 35899, USA
E-mail: jesmith@ebs330.eb.uah.edu

Twelve Co-Cu powder compact samples with different liquid volume fractions were processed during microgravity liquid phase sintering on a suborbital sounding rocket and three Space Shuttle missions. The processing times ranged from 2.5 minutes to 66 minutes. The samples exhibited dimension stability after sintering. Microstructural evolutions such as densification, dihedral angle, contact per grain and grain growth rates, indicated a dependency on Cu composition and sintering time. Grain growth analysis showed a diffusion-controlled grain growth mechanism. The diffusional layer was found in a microgravity processed 70vol%Co-Cu sample. A mechanism that explains the transient nature of this diffusion layer is proposed and used to explain the results at other processing times. Agglomeration and coalescence of particles were observed in this study, and the grain size distributions were in agreement with LSEM model, which incorporates the effect of higher solid volume fraction and particle coalescence. Analysis of the samples also revealed considerable pore formation and metamorphosis. Unlike the Fe-Cu samples, in which pore breakup was found, pore filling and coarsening dominate in all Co-Cu samples. The evolution of these parameters has been used to enhance the understanding of driving forces that contribute to the pore metamorphosis during liquid phase sintering in the Co-Cu system under microgravity.

1. Introduction

Liquid Phase Sintering (LPS) is a widely used industrial powder metallurgy process. In unit gravity processing, density differences cause sedimentation within the sample during sintering, which can produce slumping. Sedimentation contributes to solid migration, stratification, non-uniform coarsening and anisotropy in the mechanical and material properties of the sintered compacts [1–3]. Conducting LPS in microgravity provides a unique opportunity to isolate transport from sedimentation mechanisms, thereby permitting the study of transport effects on macrostructure and microstructure without many side effects [4–8].

The Co-Cu system has been studied in some detail because the density of cobalt and copper are similar so that gravitational effects in LPS are minimized [9–13]. However, even with a small (about 0.8 g/cm^3) density difference between two phases [14], it is not possible to eliminate buoyancy effects such as pore migration and differential settling in unit gravity. These are processes that can not be eliminated by density matching alone. Those effects are still present in microgravity processed samples and are functions of particle agglomeration and coalescence driven by surface tension, capillary forces and other interaction forces.

Liquid Phase Sintering (LPS) includes three overlapping stages, namely, rearrangement stage, solution-reprecipitation stage and solid state stage. Grain growth is the characteristic of the last two stages. The modeling to predict particle coarsening is technologically important because of the dependence of properties on microstructure [15]. In 1961, Lifshitz *et al.* stated (the low volume fraction theory) that the cube of the average particle radius grows proportional with annealing time if mass transport is by diffusion [16, 17]. They also showed particle size distributions in the limiting case of long annealing times. During the last decade numerous experiments have been conducted and theoretical approaches have been attempted to improve the LSW theory [1, 13, 18–21] with the focus on prolonged

sintered particles. The particle growth in rearrangement stage and solution-reprecipitation stage has been ignored as it is difficult to capture in unit gravity studies. In this paper, the recent experimental results from microgravity processed Co-Cu samples will be presented and some qualitative analysis on diffusion controlled grain growth in short sintering time will be discussed.

2. Experimental details

LPS of twelve Co-Cu powder compacts were conducted aboard the Consort sounding rocket and three Space Shuttle missions. The compositions were selected to yield 30, 40 and 50 volume percent of the liquid copper phase during sintering. The furnace module for these flights was configured to exceed the melting point (1356 K) of copper. The Co-Cu samples were processed at 1373 K for 2.5 minutes aboard the Consort 4 suborbital sounding rocket, 5 minutes aboard STS-57, 17 minutes aboard STS-60 and 66 minutes aboard STS-63, using the Equipment for Liquid Phase Sintering Experiments (ECLiPSE) flight furnace and quench system, described elsewhere [22–24]. Three different Co-Cu sample compositions were processed aboard each flight.

Co-Cu green compacts were fabricated from high purity Co and Cu powders. Co purity was 99.8% with a mean particle size of 1.6 microns. The Cu powder had an average particle size of 2 micron and a purity of 99.5%. The powders were supplied and graded by Alfa and were used as received without further modification. The Co and Cu powders were weighed in air and blended in a rotary mixer, the speed of which was optimized using the relationship $\mathrm{RPM} = 32/(\text{cylinder diameter})^{1/2}$ [25].

The mixed powders were transferred to a die lubricated with zinc stearate. A Carver hydraulic laboratory press was used to exert a compaction pressure of 110 MPa. This pressure and was applied for one hour to obtain a green compact with 70% theoretical density, without the use of internal waxes commonly used to prepare LPS compacts. The compaction pressure of 110 MPa and pressing time was selected to minimize forced shape accommodation, compact swelling, and solid skeletal formation within the compact [23]. The cylindrical compacts were of 10 mm height and 18.8 mm in diameter.

The pressed compacts were reduced in a tubular reactor under a flowing gas mixture of 5% H_2 with the balance He, following a time and temperature profile designed to remove contaminating oxides and lubricants. The samples were then separated by stainless steel shims, stacked in a cylindrical stainless steel ampoule and loaded into the flight furnace. For ground processing, the sample diameter was reduced to 12 mm and the samples loaded into alumna crucibles prior to insertion into the stainless steel ampoule.

3. Results and discussion

3.1. Dimensional stability in microgravity

The microgravity-processed Co-Cu samples were found to retain their shape even when the liquid volume fraction was as high as 50% (shown in Fig. 1b), whereas the ground processed Co-Cu sample shows distortion and slumping (Fig. 1a). This was consistent with the findings of numerous past studies of LPS in Microgravity [4, 7]. The three-phase system remained in equilibrium in orbit while the sample that was sintered on the ground displayed considerable distortion and slumping. Using the Co-Cu phase diagram, at a temperature of 1120 °C, the solubility of Co in liquid Cu is about 8.8% and the liquid solubility in solid Co is about 16%. The solubility ration is thus 0.55. The high solubility of Cu in Co will result in liquid penetration into the solid without significant dissolution of the Co grain in Cu liquid, which in turns led to a closed pore structure by which all pores are trapped inside the sample. Unlike ground processed samples, where pores were driven out due to the particle settling and buoyancy effect, the microgravity-processed samples retained the pores, thus providing a unique opportunity to study the pore metamorphosis.

3.2. Solid-liquid phase equilibrium and grain growth modeling

Grain growth occurs at the very beginning of the sintering process and throughout the entire sintering process. The major driving force for grain growth is the decrease in the interfacial energy. Smaller grains have larger chemical potential and are more soluble in the liquid phase. Therefore, smaller grains tend to dissolve and solidify on the surface of larger grains, enhancing grain

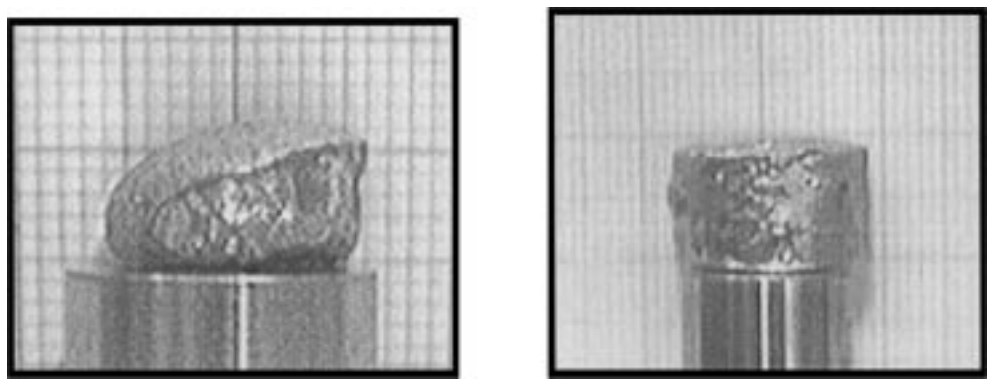

Figure 1 (a) Microgravity processed 50vol.%Co-Cu sample; (b): Ground processed 70vol.%Co-Cu sample.

growth, a process termed Ostwald ripening [26]. As a result, solute will diffuse from small to large particles through the solvent matrix.

The classical LSW theory predicts that the average radius increases asymptotically as the cube root of time. However, application of this theory is only valid for a vanishingly small volume fraction of dispersed phase in the absence of any convective contribution to mass transport and other conditions [27, 28]. So far most LPS composites were processed in unit gravity and therefore affected by the density differences between the components. In addition, most ground experiments have been limited to low solid volume fraction [9–12]. The microgravity samples discussed below have high solid volume fractions from 50vol%Co to 70vol%Co. The effect of composition and processing time on the grain size for these samples is shown in Fig. 2. The data were fitted to a first order function that represented the best fit. In those figures, the cube of the grain sizes is plotted against the processing time. The linear grain growth rate shows diffusion controlled grain growth. The rate of grain growth increases with decreasing volume fraction of the liquid phase. This was consistent with previous LPS studies of prolonged sintered samples that showed an increase in the rate of grain growth with increasing grain contact. The interesting part of those figures is that the extension of the three-grain growth lines converges on a single point (Fig. 2). The grain size at this point is larger than the grain size of the green compact (unsintered compacts). This suggests that, solid state sintering began before the melt and, secondly, there is a critical temperature where grain growth in solid-state sintering is independent of the solid volume fraction. An examination of Fig. 5 shows that the grain growth rate increases as the liquid volume fraction was decreased. This indicated that a smaller separation distance (small length scale) between the grains enhances the mass flux between particles and thus increases the ripening rate.

The settling of solid particles in unit gravity complicates the experimental evaluations of coarsening theories. Effects of slumping and particle settling also contribute to the anisotropic sintering which results in uneven local solid volume fraction and non-uniform particle coarsening [2, 3, 29]. The ground test on the Co-Cu system has been published by some researchers with different results. In ground processed samples, agglomeration and coalescence were mainly attributed to sedimentation by gravitational force, which led to pore evacuation and high grain growth rate. The agglomeration in higher solid volume fraction samples may cause the local solid volume to exceed the limit where solid skeleton formation occurs. This may lead to similar grain growth rate for different solid volume fraction samples.

Even in microgravity where sedimentation driven rearrangement is minimized, agglomeration due to the weak interaction forces still exists [30]. Other process, such as particle wetting, liquid penetration due to the surface tension, pore filling, or liquid ejection also attribute to the agglomeration. Fig. 3 shows an agglomerated particle zone adjacent to a liquid copper pool formed by liquid ejection. Observations on different solid volume fraction samples showed a decrease in tendency on agglomeration as solid volume fraction increased. This appears to be reasonable because Cu has higher solubility in Co and a skeletal structure is easy to generate in higher solid volume fraction samples, which prohibited further agglomeration.

Given the extent of agglomeration, diffusion controlled grain growth appears to be affected by the local solid volume fraction. For a first approximation, the solid volume fraction can be calculated by an equation derived by German *et al*. [31], relation the volume fraction of solid, the three-dimensional coordination number and dihedral angle:

$$V_s = -0.831 + 0.806N_c - 0.0555N_c^2 + 0.00176N_c^3 - 0.355N_c \cos\left(\frac{ø}{2}\right) + 0.00803\left[N_c \cos\left(\frac{ø}{2}\right)\right]^2$$

where V_s is the volume fraction of solid, N_c is the three-dimensional coordination number, and ø is the dihedral angle. This equation was developed using computer simulations of idealized liquid phase sintered microstructures. The calculated solid volume fraction

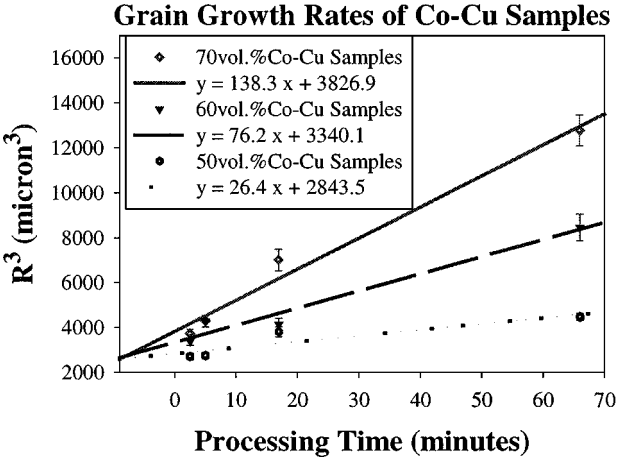

Figure 2 The effects of sintering time and solid volume fraction on grain growth of Co-Cu samples. As shown in this figure, three grain growth lines converge on one point.

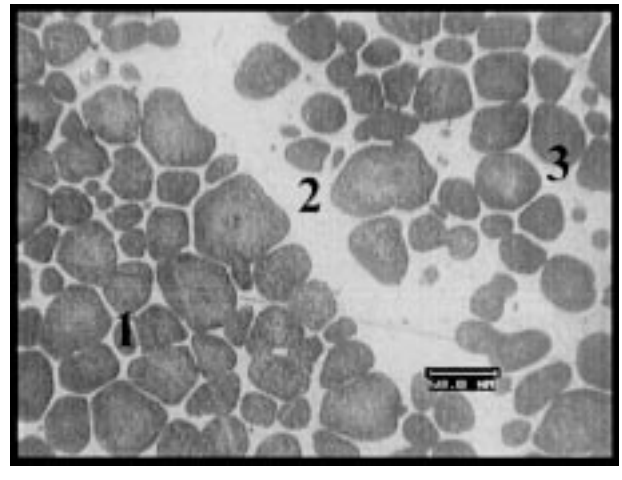

Figure 3 Agglomeration in microgravity processed Co-Cu sample. (1) Closed packed particles; (2) Liquid copper pool; (3) Loosely packed particle zone.

TABLE I Calculated solid volume fraction of sintered Co-Cu samples

Initial Solid Volume Fraction	70vol.% Co	70vol.% Co	70vol.% Co	70vol.% Co
Processing Time (minutes)	2.5	5	17	66
Calculated Solid Volume Fraction	0.848	0.846	0.829	0.770
Initial Solid Volume Fraction	60vol.% Co	60vol.% Co	60vol.% Co	60vol.% Co
Processing Time (minutes)	2.5	5	17	66
Calculated Solid Volume Fraction	0.778	0.779	0.779	0.765
Initial Solid Volume Fraction	50vol.% Co	50vol.% Co	50vol.% Co	50vol.% Co
Processing Time (minutes)	2.5	5	17	66
Calculated Solid Volume Fraction	0.749	0.744	0.760	0.677

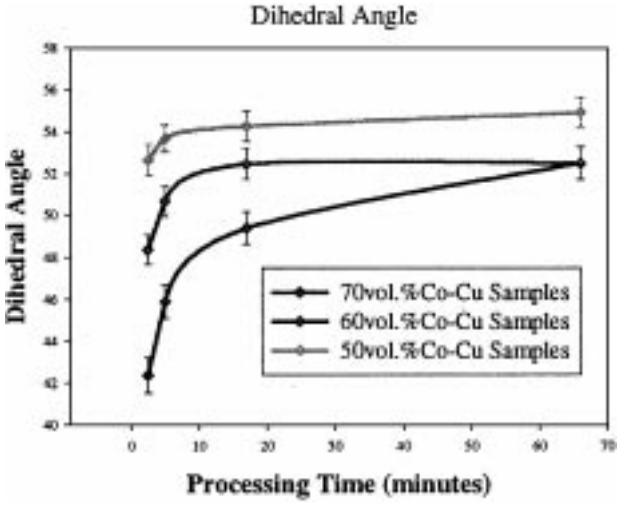

Figure 4 Effects of solid composition and sintering time on dihedral angle of microgravity processed Co-Cu samples.

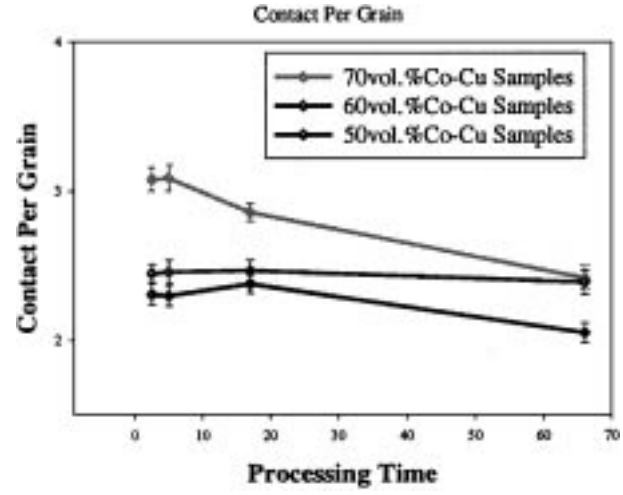

Figure 5 Effects of solid composition and sintering time on contact per grain of microgravity processed Co-Cu samples.

after agglomeration is shown in Table I. Those numbers can be used as a local solid volume fraction.

The effect of composition and sintering time on the dihedral angle measured in the Co-Cu system is shown in Fig. 4. The dihedral angles increase with processing time. As would be expected, the initial values for the dihedral angle are higher for the samples with higher liquid volume fractions. The interesting observation is that the dihedral angles appear to converge to an equilibrium value of about 55°, consistent with similar observations in studies using the Fe-Cu system [4].

The effects of composition and processing time on the number of contacts per grain were shown in Fig. 5. The three dimension coordination number can be calculated from contact per grain values using equation given by German [31]:

$$N_c = \frac{C_g}{0.805 \sin \frac{ø}{2}}$$

where C_g is the value of contact per grain and ø is the dihedral angle. The number of contacts per grain decreased with increasing volume fraction of liquid as would be expected. The number of contacts per grain displayed little change during the initial stages of LPS under microgravity. However, the microstructure of these samples from the initial stages of LPS showed the existence of liquid pools (Fig. 3). This is also indicative of agglomeration that ensures consistency in the number of contacts per grain. Any substantial decrease in this number is a result of grain growth in the later stages of LPS.

Based on LSW theory, the asymptotic normalized particle size distribution of the solid phase can be predicted. However, the assumption of vanishingly small solid volume fraction makes it improper for high solid volume liquid phase sintered samples. Davies *et al.* modified the LSW model to include the effect of solid volume fraction and the encounter of particles, which is call LSEM model [32]. Their predicted distributions were wider than those predicted by LSW model and the distribution is proportional to the solid volume fraction. Based on LSEM model and solid volume fraction, the predicted solid volume fractions are plotted for all 12 Co-Cu samples with the measured particle size distribution. Figs 6, 7, and 11 show the grain size distribution as a function of solid composition for samples processed for 66 minutes and Figs 8–11 show the grain size distribution as a function of processing time for 70vol%Co-Cu samples. In comparing with LSW, the particle size distributions based on LSW model are also plotted. It can be seen that the LSW model doesn't correlate well with the measured particle size distribution while the LSEM model does. This is consistent with similar observations in the Fe-Cu system [30].

Due to the agglomeration in Co-Cu samples, the grain growth appears to be driven by diffusion and grain coalescence, which can be expressed as [19]:

$$R^3 - R_0^3 = (k_d + k_c)t$$

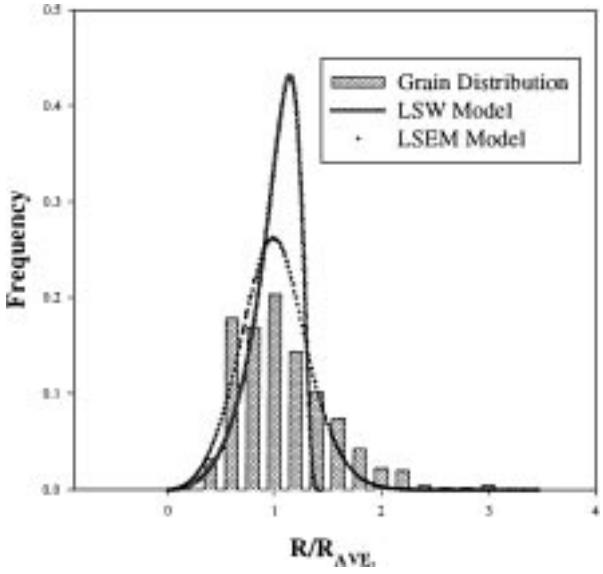

Figure 6 Grain size distribution of 50vol.% Co-Cu sample (processing time 66 minutes).

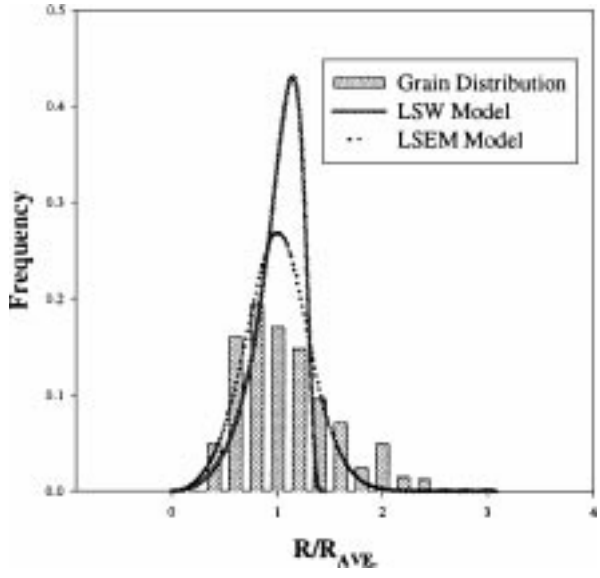

Figure 7 Grain size distribution of 60vol.% Co-Cu sample (processing time 66 minutes).

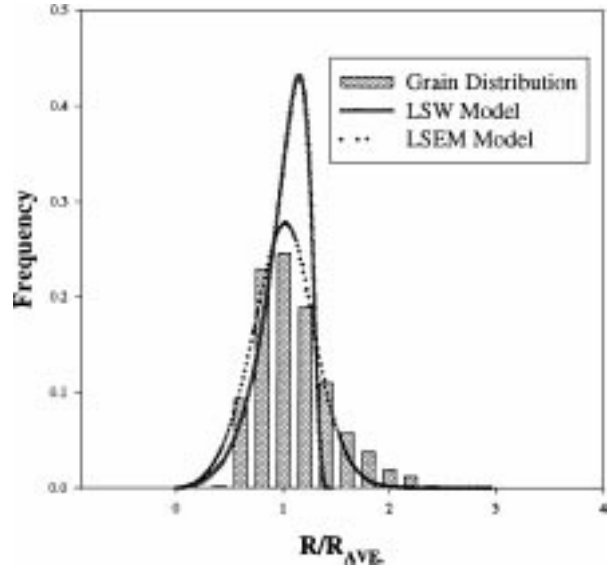

Figure 8 Grain size distribution of 70vol.% Co-Cu sample (processing time 2.5 minutes).

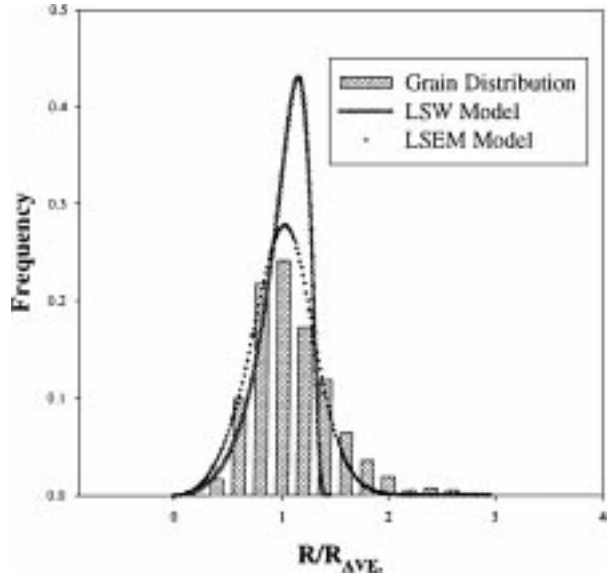

Figure 9 Grain size distribution of 70vol.% Co-Cu sample (processing time 5 minutes).

where R_0 and R is the average grain size before and after sintering, k_d is the diffusion coefficient and k_c is the coalescence coefficient. However, detailed microstructure analysis shows that two kinds of diffusion mechanisms exist for short sintering time. Fig. 12 shows a SEM photograph of Co grains processed in microgravity for 17 minutes. Two diffusion layers exist which were never captured in either very short or prolonged sintered samples. The two different layers shown by different gray scale are separated by dark grain boundaries. X-ray diffraction studies indicated different Cu compositions between the two layers and between the inner core and outer liquid phase regions. The outer layer has a higher Cu concentration than the inner layer. Comparing to the Co-Cu phase diagram, one possible explanation is that the outer layer is formed by solution reprecipitation and inner is formed directly from Cu-Co solid-phase diffusion forming the solid solution phase. Examination of the phase diagram shows that initially, the Co particles must dissolve to saturate the Cu-rich phase, a rapid process. While this process is occurring, solid-state diffusion is occurring within the Co grain to form the solid solution. In addition, Ostwald Ripening occurs from the liquid matrix during the growth phase. For such system with a substantial solid-solution phase, the grain growth rate function may need to be expressed in some form such as:

$$R^3 - R_0^3 = (k_{d1} + k_c)t + k_{d2}t'$$

where R_0 and R is the average grain size before and after sintering, k_{d1} is the diffusion coefficient of cobalt in copper, k_{d2} is the diffusion coefficient of copper in cobalt and k_c is the coalescence coefficient, and t' is the time for copper to saturate cobalt.

To model this behavior, we applied the shrinking core model [33]. Assuming a spherical cobalt particle with

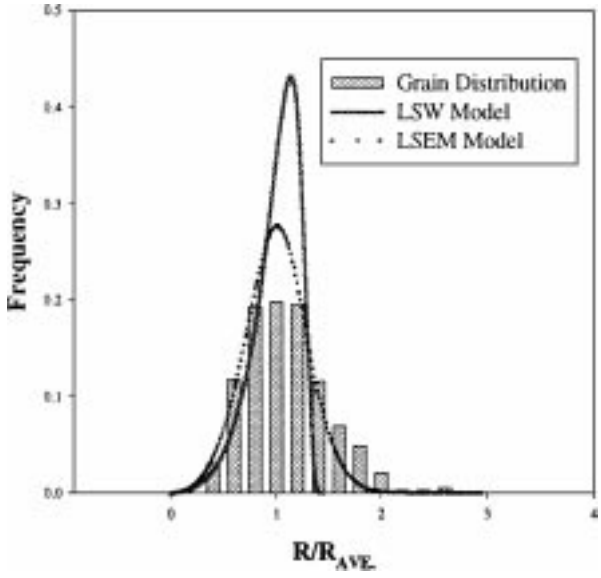

Figure 10 Grain size distribution of 70vol.% Co-Cu sample (processing time 17 minutes).

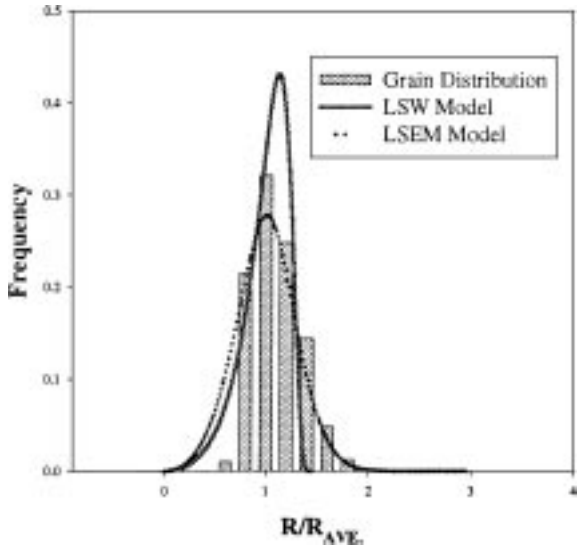

Figure 11 Grain size distribution of 70vol.% Co-Cu sample (processing time 66 minutes).

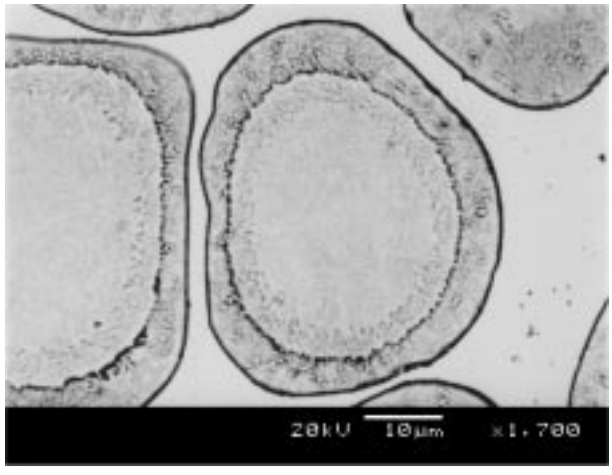

Figure 12 Diffusion layers in a Co grain (70vol%Co-Cu sample, processing time 17 minutes).

radius R dispersed in liquid copper, the diffusion flux of species u can be expressed as [34, 35]:

$$\frac{\partial u}{\partial t} = \frac{\mathrm{D}\partial^2 u}{\partial x^2} \quad \text{with} \quad 0 \le x \le R \tag{1}$$

The copper concentration (C_1) anywhere inside the cobalt particle at time t can be calculated using the model solution;

$$\frac{C_1}{C_0} = 1 + \frac{2}{\pi\xi}\sum_{n=0}^{\infty}\frac{(-1)^n}{n}\exp[-n^2\pi^2\xi T]\sin[n\pi\xi] \tag{2}$$

where C_0 is the Cu concentration at boundary, ξ is the dimensionless parameter, $\xi = r/R.$, T is the dimensionless time, $T = \mathrm{D}t/R^2$. The diffusion coefficient of cobalt in liquid copper is 4.0968×10^{-9} m^2/s [36] while the diffusion coefficient for copper in solid cobalt is approximated as 1.905×10^{-14} m^2/s. Using these diffusion coefficients, it takes less than one second for cobalt to saturate the liquid copper by dissolution, while it takes 33 minutes for copper to reach 95% saturation in cobalt particle using a 20 micron initial diameter. This suggests that, during liquid phase sintering, right after liquid formation, the liquid copper became saturated with cobalt very quickly, decreasing the initial diameter of the cobalt particle. Then copper atoms start to slowly penetrate into the cobalt particles. For very short time sintering (less than 5 minutes), no layers was observed since they may be too thin. In addition, for samples after 66 minutes of sintering, only a homogeneous fully saturated cobalt layer was observed. These findings support our mechanism.

3.3. Pore metamorphosis

Unlike Fe-Cu samples, where pore breakup dominated in short time sintering (<5 minutes) and pore coarsening in longer time sintering (>17 minutes), pore filling and coarsening were observed in Co-Cu samples. During the initial stages of LPS, because of the low solubility ratio, liquid copper wets the Co particles dissolving them. Since the green compact has some initial porosity, about 30%, pores coalesce within the compact during the melt. These pores obtain a size that cannot be destabilized by the presence of the solid particles. These pores eventually become surrounded by particles that distort the liquid-vapor interface.

Consider a pore that is surrounded by solid particles that bound together by capillary forces induced by the liquid phase. As the particles grow, the radius of the liquid meniscus between particles increase. As a result of this growth, a pressure difference draws liquid into the pore, thus reducing the pore radius and increasing densification. The mechanics of pore filing have been discussed by Park [9, 10], using ground processed Co-Cu and Fe-Cu as experimental systems. Fig. 13 shows a representative microstructure of two filled pores similar to those observed by Park *et al*. A given pore size requires a critical particle size to induce pore filling. Grain growth and the initial particle size would therefore be important factors controlling pore filling and the

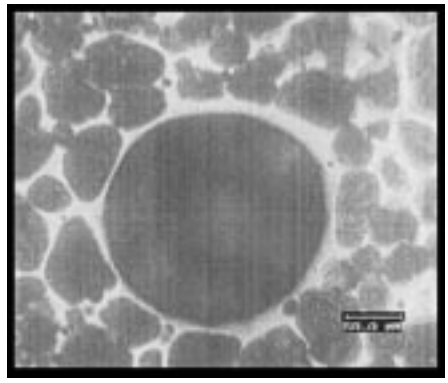

Figure 13 Pore filling in a Co-Cu sample.

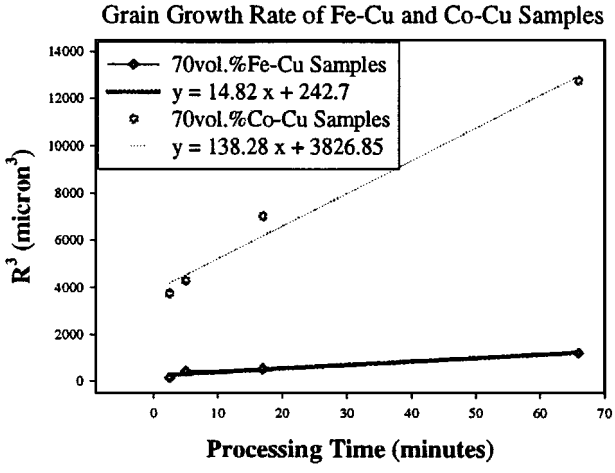

Figure 14 Grain growth comparison between Fe-30%Cu and Co-30%Cu samples (y is the cube of grain radius, x is the sintering time).

extent of pore filling would be dictated by the rate of grain growth, solubility between the phases and initial sizes of the pores. Comparing the grain growth rates in Fe-30%Cu and Co-30%Cu samples in microgravity, see Fig. 14, a grain growth constant of 14.8 and 138 is found for Fe-30%Cu and Co-30%Cu, respectively. It is most likely that this difference is responsible for the differences in pore behavior observed in the two systems. Further work on the pore metamorphosis in microgravity will be presented soon to clarify the mechanics of these differences in behavior.

Similar to particle growth, pore coarsening due to Ostwald ripening is also observed. For different solid volume fraction samples, as the sintering time increased, the total number of pores observed decreased and the size of pore increased. Pore filling in the Co-Cu system was considerably more significant than that in the Fe-Cu system [4].

3.4. Densification

Densification is an important aspect of all LPS manufacturing operations. The elimination of pores and the production of a fully dense compact are the goal of all powder metallurgical processes with the exception of the production of porous materials. Higher densification also implies higher amounts of shrinkage during processing. The normalized linear and volumetric dimensional changes, $\Delta L/L_0$ and $\Delta V/V_0$ are commonly used to record densification. The normalized volumetric shrinkage (densification) for the Co-30%Cu, Co-40%Cu and Co-50%Cu samples as a function of time are presented in Fig. 15.

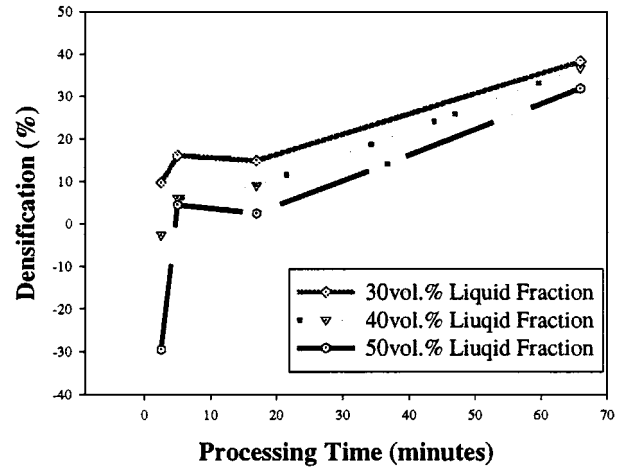

Figure 15 Effects of solid composition and sintering time on densification of microgravity processed samples.

The densification data for Co-50%Cu samples shows that the sample sintered for 2.5 minutes exhibited the maximum amount of swelling. However, an increase in the processing time to 5 minutes resulted in a rapid increase in densification. Further increases in the processing time resulted in a decrease in the rate of densification that reached a value of only 40% after 66 minutes. The densification of Co-40%Cu after 2.5 minutes of LPS is significantly higher than that of Co-50%Cu. However, after 5 minutes of LPS, the densification rates for the Co-40%Cu and Co-50%Cu are comparable.

The densification rates in the Co-30%Cu do not change much with time indicating that the rearrangement phase of LPS lasted for only a short period of time when compared to the Co-50%Cu sample. The similarity in the densification rates for the Co-30%Cu and Co-50%Cu samples after 17 minutes suggests that the dominant factor in the densification of Co-Cu occurs in the later stages of LPS.

Several factors are relevant to the observed differences in the densification behavior, particularly in the early stages of LPS under microgravity. Considering the mutual solubilities of Co and Cu, swelling would be expected in these samples following melting of Cu and wetting of the Co particles. The initial swelling would be followed by the rearrangement phase of LPS. Densification results indicate that rearrangement is significant in Co-50%Cu sample as compared to the Co-30%Cu and Co-40%Cu samples. A previous study [30] of LPS in the Fe-Cu system under microgravity indicated similar behavior that was attributed to agglomeration of the Fe particles. It appears likely that a similar agglomeration phenomenon is responsible for this initial rapid increase in the rate of densification observed in the Co-50%Cu sample. Agglomeration appears more pronounced in samples with high volume fractions of liquid since particle mobility is the highest. Another relevant factor is pore filling which would also be expected to cause rapid densification in

the early stages of LPS. However, this would be highly dependent on the Co particles attaining the critical grain size to induce filling as discussed by Park [9]. Diffusion would dominate densification in the later stages of LPS and, as observed in this study, does not contribute significantly.

4. Conclusion

The effects of composition and sintering time on various properties of microgravity processed liquid phase sintered Co-Cu samples was presented, such as densification, pore metamorphosis, grain size, grain growth rate, dihedral angle, contact per grain and grain size distribution. The unique μg environment enables the mechanistic and kinetic studies of grain growth and pore formation. Cobalt grain growth during LPS in microgravity shows a diffusion-controlled mechanism. The cube of grain size is proportional to the sintering time. The solid volume fraction and sintering time affect the grain growth rate and the particle size, which is different from some ground sintering results [13]. The diffusion layer was observed during the analysis for the first time, which provide direct evidence for the diffusion controlled grain growth. The shrinking core model can be used to model the diffusion processing during short time sintering and more studies needs to be done in order to fully understand this phenomena. Pore fillings and pore coarsening was also observed. Combining with pore behavior in Fe-Cu samples, A new pore metamorphosis mechanism may be in effect.

Acknowledgment

This work was supported by NASA and the Consortium for Materials Development in Space at the University of Alabama in Huntsville under contract NAGW-812. WYLE Laboratories and Nextek Inc. are also graciously acknowledged for their involvement. Numerous individuals from both academia and corporate industrial partners have contributed their knowledge, cooperation and support to this project for which the ECLiPSE team is indeed very grateful.

References

1. R. M. GERMAN, "Liquid Phase Sintering" (Plenum Press, New York, 1985).
2. C. M. KIPPHUT, A. BOSE, S. FAROOQ and R. M. GERMAN, *Metallurgical Transactions A* **19A** (1988) 1905.
3. T. H. COURTNEY, *Scripta Met.* **35**(5) (1996) 567.
4. Z. XUE, Master thesis, University of Alabama in Huntsville, 1995.
5. Z. XUE, S. NOOJIN, J. G. VANDEGRIFT and A. K. KURUVILLA, in "Experimental Methods for Microgravity Materials Science," edited by Robert Schiffman (TMS Publications, 1996), in press.
6. *Idem., High Temperatures-High Pressures* **29** (1997) 349.
7. Z. XUE, J. G. VANDEGRIFT and A. K. KURUVILLA, *Mater. Trans., JIM* **37** (1996) 1084.
8. Y. HE, S. YE, A. K. KURUVILLA and J. E. SMITH JR., in 9th International Symposium on Experimental Methods for Microgravity Materials Science, compiled and edited by Dr. Robert A. Schiffman, 1997, TMS publication (in CD-ROM format).
9. H. PARK, S. CHO and D. YOON, *Metallurgical Transactions A.* **15A** (1984) 1075.
10. H. PARK, O. KWON and D. YOON, *ibid.* **17A** (1986) 1915.
11. C. KANG and D. YOON, *ibid.* **12A** (1981) 65.
12. S. KANG and D. YOON, *ibid.* **13A** (1982) 1405.
13. W. BENDER and L. RATKE, *Acta Mater.* **46**(4) (1998) 1125.
14. D. R. LIDE (editor-in-chief), "CRC Handbook of Chemistry and Physics," 72nd ed. (CRC Press, Boca Raton, Ann Arbor, Boston, 1991–1992).
15. S. P. MARSH and M. F. GLICKSMAN, "Modeling of Coarsening and Grain Growth" (TMS Publication, 1992) p. 1.
16. I. LIFSHITZ and V. SLYOZOV, *J. Phys. Chem. Solids* **19** (1961) 35.
17. C. WAGNER, *Z. Elektrochemie* **65** (1961) 581.
18. R. M. GERMAN, Y. LIU and A. GRIFFO, *Metall. Mater. Trans.* **28A** (1997) 215.
19. Y. MASUDA and R. WATANABE, in "Sintering Processes," edited by G. C. Kuczynski (Plenum, Press, New York, 1979).
20. S. P. MARSH and C. S. PANDE, "Modeling of Coarsening and Grain Growth" (TMS Publication, 1992).
21. I. ANDERSEN, O. GRONG and N. RYUM, *Acta Metall.Mater.* **43**(7) (1995) 2689.
22. J. G. VANDEGRIFT, S. NOOJIN, K. RYAN and Z. XUE, in 7th International Symposium on Experimental Methods for Microgravity Materials Science, edited by R. Schiffman p. 79 (TMS Publications, 1995).
23. S. NOOJIN, Master thesis, University of Alabama in Huntsville, 1993.
24. S. NOOJIN, J. G. VANDEGRIFT, K. HARTMAN and J. E. SMITH, JR., ASME Heat Transfer Div. Pub., Vol. HTD 259, p. 127, 1993.
25. R. M. GERMAN, "Powder Metallurgy Science" (Metal Powder Industries Federation, Princeton, New Jersey, 1984).
26. W. OSTWALD, *Z. Phys. Chem.* **34** (1900) 495.
27. L. RATKE, "in Progr. Astronautics, Vol. 130: Low-Gravity Fluid Dynamics and Transport Phenomena," edited by J. N. Koster and R. L. Sani (AIAA, Washingto, 1990) p. 661.
28. P. VOORHEES, *J. Statist. Phys.* **38** (1985) 231.
29. S. S. MANI, R. M. GERMAN, *Adv. In Powder Metal.*, **1** (1990) 453.
30. J. NASER, A. K. KURUVILLA and J. E. SMITH, JR., *Journal of Materials Science* **33** (1998) 5573.
31. S. YANG and R. M. GERMAN, *Metallurgical Transactions A.*, **22A** (1991) 786.
32. C. K. L. DAVIES, D. NASH and R. N. STEVENS, *Acta. Metal.* **28** (1980) 179.
33. G. F. FROMENT and K. B. BISCHOFF, "Chemical Reactor Analysis and Design," 2nd ed. (John Wiley & Sons, Inc., 1990).
34. J. CRANK, "The Mathematics of Diffusion" (Oxford University Press, 1975).
35. H. S. CARSLAW and J. C. JAEGER, "Conduction of Heat in Solids" (Oxford University Press, 1959).
36. D. B. BUTRYMOWICZ, J. R. MANNING and M. E. READ, "Diffusion Rate Data and Mass Transport Phenomena for Copper Systems" (International Copper Research Association, Inc., 1977).

Received 2 July 1999
and accepted 1 May 2000